BIOCHEMISTRY
including biophysical chemistry & molecular biology

Article

pubs.acs.org/biochemistry

The Benefits of Being β-Crystallin Heteromers: βB1-Crystallin Protects βA3-Crystallin against Aggregation during Co-refolding

Sha Wang, Xiao-Yao Leng, and Yong-Bin Yan*

State Key Laboratory of Biomembrane and Membrane Biotechnology, School of Life Sciences, Tsinghua University, Beijing 100084, China

ABSTRACT: β-Crystallins are the major structural proteins in mammalian lens, and their stability is critical in maintaining the transparency and refraction index of the lens. Among the seven β-crystallins, βA3-crystallin and βB1-crystallin, an acidic and a basic β-crystallin, respectively, can form heteromers *in vivo*. However, the physiological roles of the heteromer have not been fully elucidated. In this research, we studied whether the basic β-crystallin facilitates the folding of acidic β-crystallin. Equilibrium folding studies revealed that the βA3-crystallin and βB1-crystallin homomers and the βA3/βB1-crystallin heteromer all undergo similar five-state folding pathways which include one dimeric and two monomeric intermediates. βA3-Crystallin was found to be the most unstable among the three proteins, and the transition curve of βA3/βB1-crystallin was close to that of βB1-crystallin. The dimeric intermediate may be a critical determinant in the aggregation process and thus is crucial to the lifelong stability of the β-crystallins. A comparison of the Gibbs free energy of the equilibrium folding suggested that the formation of heteromer contributed to the stabilization of the dimer interface. On the other hand, βA3-crystallin, the only protein whose refolding is challenged by serious aggregation, can be protected by βB1-crystallin in a dose-dependent manner during the kinetic co-refolding. However, the protection is not observed in the presence of the pre-existed well-folded βB1-crystallin. These findings suggested that the formation of β-crystallin heteromers not only stabilizes the unstable acidic β-crystallin but also protects them against aggregation during refolding from the stress-denatured states.

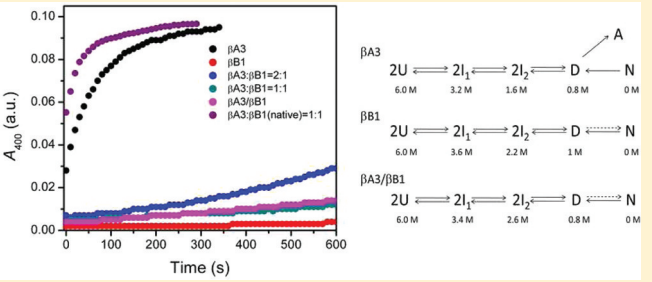

Cataract, the most common cause of vision loss in human beings, is a protein conformational disease due to the accumulation of insoluble proteins that obstruct the passage of light through the lens.[1−3] The major component of insoluble proteins in cataract is crystallins,[3−7] which are also the major structural proteins in the lens of eye.[8−10] The high concentration and short-range order of various crystallins ensure the transparency and refraction of lens.[10,11] Human lens proteins contain three classes of crystallin:[12] α-crystallin, a heteropolymer serves as a chaperone;[13,14] β-crystallin, a complex mixture of oligomers;[15] and γ-crystallin, a monomeric structural protein family. These proteins should be extremely stable in lens since the mature lens cell lasts an individual a lifetime with no protein turnover. As age increases, crystallins gradually lose solubility and stability in the persistent presence of environmental stresses, and their aggregation finally leads to light scattering, which is generally recognized as the main cause of cataract.[3,11] Meanwhile, congenital cataract-linked mutations usually destabilize crystallins without interference of the folding pathway.[3,16,17] Therefore, the understanding of crystallin stability and folding pathway is of great importance to reveal the mechanism of cataract and also to provide valuable implications for studying other folding diseases.

Among the three crystallin families, β-crystallin is a widely distributed structural protein family that assembles to a wide spectrum of oligomeric states across the lens.[12] The components of β-crystallin in lens include acidic β-crystallins (βA1−βA4) and basic β-crystallins (βB1−βB3). These β-crystallins naturally associate into many heterogeneous oligomers with the sizes in the range 50−200 kDa and the dissociation constants at the micromolar level.[18] Except for being the structural protein in the lens,[15,18−20] most crystallins are expressed in tissues outside the lens, suggesting that they may also have other function. Particularly, βA3/A1-crystallin has recently been identified to be a binding partner of cathepsin D in the lysosome of the retinal pigmented epithelium.[21] The β- and γ-crystallins form the βγ-crystallin superfamily and share a conserved tertiary structure, which contains four Greek-key motifs divided into two domains.[22−25]

Denaturant-induced unfolding of several β- and γ-crystallins have been extensively studied.[26−29] Both β- and γ-crystallins are highly stable according to thermodynamic calculation.[12] β-Crystallin has been proposed to have higher stability due to its higher order oligomerization.[26] However, some γ-crystallins are found to be much more stable than the β-crystallin homodimers,[12] suggesting that the oligomeric states may not be a key determinant in crystallin stability. The high structural conservation and the large dissociation constants of β-crystallin imply that β- and γ-crystallins might undergo similar folding pathway.

Received: August 31, 2011
Revised: October 25, 2011
Published: October 27, 2011

The urea- or guanidine hydrochloride (GdnHCl)-induced unfolding of β- and γ-crystallins is suggested to follow either a two-state or a three-state model,[12] but the unfolding pathway of βB1-crystallin is proposed to contain more than one intermediate.[28] It is unclear yet whether the difference in the folding mechanism is caused by the dissimilarity in the proteins or the accuracy of experiments. Moreover, the urea-induced unfolding of βA3-crystallin was found to have a relatively lower thermodynamic stability and a higher aggregation tendency than βB1-crystallin.[22] However, although all β-crystallins, except for βB2-crystallin, form heteromers in the lens, little is known about the folding of naturally formed heterogeneous oligomers of β-crystallin. The details of the structural changes during β-crystallin folding and unfolding also remain elusive.

In human lens, both α- and β-crystallins mainly exist as heteromers, and several previous studies have tried to explore the benefits of the formation of the evolution-selected β-crystallin heteromers. It has been shown that the acidic β-crystallins are stabilized in the heteromers when subjected to heat- or urea-induced denaturation.[19,22,30,31] Moreover, βB1- and βB3-crystallin genes are expressed early during lens development.[12] An interesting question is whether the pre-existed basic β-crystallins favors the folding of acidic β-crystallins. In this research, this question was addressed by comparing the GdnHCl-induced unfolding and refolding pathways of βA3- and βB1-crystallins as well as their heteromer βA3/βB1-crystallin. The βA3- and βB1-crystallins were chosen as the model system according to their high expression level in human lens and their abundance in the β-crystallin heteromers. Our results clearly showed that the three β-crystallins all follow multistate folding processes, among which the folding process of βA3/βB1-crystallin is similar to that of βB1. Interestingly, we found that βB1-crystallin can successfully protect βA3-crystallin against aggregation during co-refolding, but the pre-existed well-folded βB1-crystallin could not.

MATERIALS AND METHODS

Chemicals. GdnHCl, 8-anilino-1-naphthalenesulfonic acid (ANS), and sodium dodecyl sulfate (SDS) were purchased form Sigma Chemical Co. All other chemicals were local products of analytical grade.

Protein Expression and Purification. The His-tagged recombinant βB1- and βA3-crystallins were overexpressed in *Escherichia coli* BL21 with pET28a plasmid and purified by Ni-NTA affinity column and gel filtration chromatography as described previously.[31] The βA3/βB1-crystallin heteromer was prepared by incubating equimolar of βB1-crystallin and βA3-crystallin at 37 °C for 2 h, and the formation of heteromer βA3/βB1-crystallin was identified by size-exclusion chromatography (SEC) and SDS-PAGE analysis. The protein concentration was determined according to the Bradford method using bovine serum albumin as a standard.[32]

Protein Unfolding and Refolding. The unfolding experiments of the three proteins were performed by incubating the purified proteins in buffer A (20 mM sodium phosphate buffer, 0.15 M NaCl, 1 mM EDTA, 1 mM DTT, pH 7.2) containing different concentrations of GdnHCl for 16 h at 4 °C. As for the refolding experiments, the purified proteins were fully denatured in 6 M GdnHCl for 12 h. Then the equilibrium refolding was carried out by dilution of the denatured samples in buffer A with the final concentrations of GdnHCl varied from 0.2 to 6 M at 25 °C for 24 h. The final protein concentration was 0.2 mg/mL for both the unfolding and refolding experiments.

Spectroscopic Experiments. All spectroscopic experiments were performed at 25 °C with a protein concentration of 0.2 mg/mL. The fluorescence spectra were measured on an F-2500 fluorescence spectrophotometer (Hitachi Ltd., Tokyo, Japan) with a 5 nm slit width for both excitation and emission. The intrinsic fluorescence was measured with an excitation wavelength of 295 nm and an emission wavelength ranging from 300 to 400 nm. The extrinsic ANS fluorescence of crystallins at various concentration of GdnHCl was monitored with an excitation wavelength of 380 nm and an emission wavelength ranging from 400 to 600 nm. The final concentration of ANS was 20 μM. The circular dichroism (CD) spectra were recorded on a Jasco J-715 spectropolarimeter (Jasco Corp., Tokyo, Japan) with a 1 mm path length cell over a wavelength range of 190−250 nm. The resultant spectra were obtained by the subtraction of the spectra of the corresponding buffers. The parameter A, which is the ratio of the intensity at 320 nm to that at 365 nm of the intrinsic fluorescence (I_{320}/I_{365}), is the characteristic of the shape and position of the fluorescence spectrum.[33,34] The phase diagram analysis of the intrinsic fluorescence, which is a sensitive tool to detect the folding intermediates,[35] was carried out as described previously.[36,37]

Aggregation Experiments. Details regarding the aggregation experiments were the same as those described previously.[38] The time-course aggregation during refolding was recorded immediately after the refolding was initiated by a fast manual dilution of the GdnHCl-denatured β-crystallins into buffer A at 25 °C. It has been proposed that the light scattering intensity is proportional to the amount of the protein in the aggregated form,[39] thus the turbidity of the proteins during unfolding was monitored by recording the absorbance at 400 nm on an Ultraspec 4300 pro UV/vis spectrophotometer from Amersham Pharmacia Biotech (Uppsala, Sweden). The final protein concentration was 0.1 or 0.2 mg/mL.

Size-Exclusion Chromatography. The size-exclusion chromatography (SEC) analysis of the samples was the same as described previously.[40] In brief, the gel filtration experiments were carried out on a Superdex 75HR 10/30 column on an AKTA FPLC (Amersham Pharmacia Biotech, Sweden). The column was pre-equilibrated with buffer A containing the given concentrations of GdnHCl, and then about 100 μL protein solutions were injected into the column. All samples were run at a flow rate of 0.5 mL/min at 16 °C. The elution peaks were collected for further identification by SDS−polyacrylamide gel electrophoresis (SDS-PAGE) using 12.5% separating gel in the reducing conditions. Silver staining was performed according to the standard protocol.[41]

Data Analysis. The equilibrium folding transition curves monitored by parameter A was analyzed according to a three-state model as characterized previously.[26,42]

$$N_2 \leftrightarrow 2I \leftrightarrow 2U \quad (1)$$

where N_2 is the native protein, I is the monomeric intermediate state, and U is the fully unfolded state. The equilibrium constants for the three transitions in eq 1 are

$$K_{NI} = [I]^2/[N_2], \quad K_{IU} = [U]/[I] \quad (2)$$

and the mole fractions of each species are

$$f_I = [I]/P, \quad f_N = 2[N_2]/P = 2Pf_I^2/K_1, \quad f_U = [U]/P = f_I K_2 \quad (3)$$

$$f_N + f_I + f_U = 2Pf_I^2/K_1 + f_I + f_I K_2 = 1 \quad (4)$$

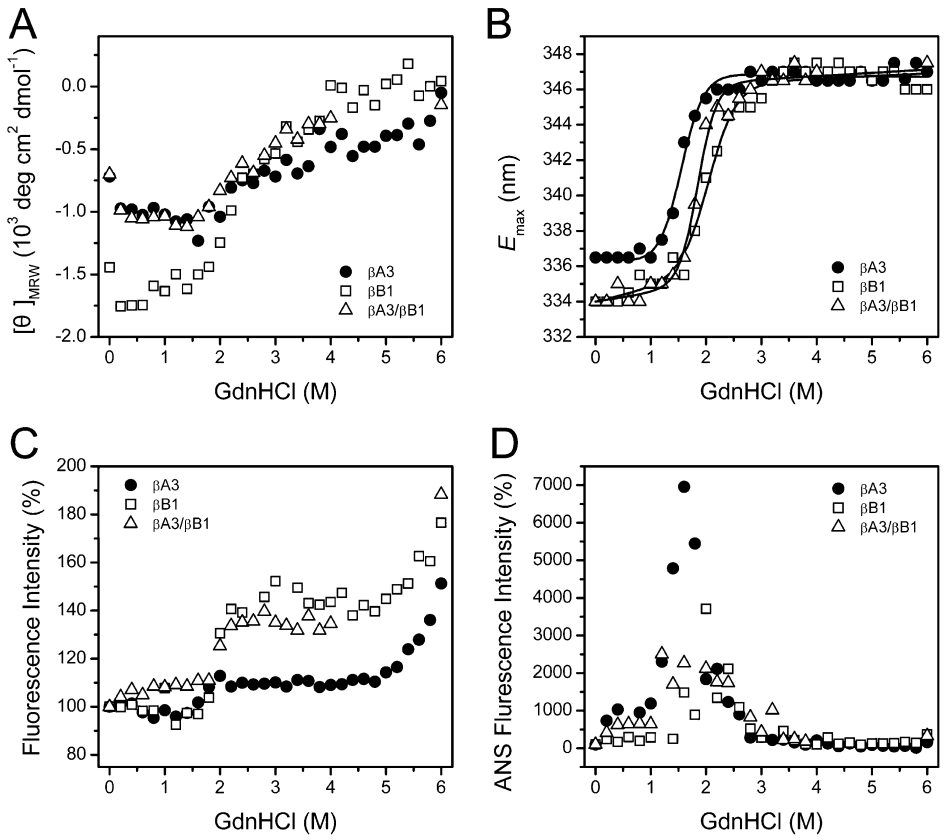

Figure 1. Unfolding transition curves of βA3- (filled cycles), βB1- (open square), and βA3/βB1-crystallins (open triangle) monitored by the ellipticity at 222 nm (A), the emission maximum wavelength (B), and the intensity (C) of the intrinsic Trp fluorescence and the ANS fluorescence intensity at 470 nm (D). For the unfolding experiments, the protein was incubated in buffer A in the presence of various concentrations of GdnHCl for 12 h at 4 °C. The final protein concentration was 0.2 mg/mL. All spectroscopic experiments were carried out at 25 °C.

The quadratic equation (eq 4) is solved, which yield f_I:

$$f_I = -b + \sqrt{b^2 - 4ac}/2a \quad (5)$$

in which

$$a = 2P, \quad b = K_1(1 + K_2), \quad c = -K_1$$

The free energy changes can be expressed as a function of the GdnHCl concentration:

$$\Delta G_{NI} = -RT \ln K_{NI} = \Delta G_{NI}^{H_2O} - m_{NI}[\text{GdnHCl}] \quad (6)$$

$$\Delta G_{IU} = -RT \ln K_{IU} = \Delta G_{IU}^{H_2O} - m_{IU}[\text{GdnHCl}] \quad (7)$$

$$\Delta G_{NU}^{H_2O} = \Delta G_{NI}^{H_2O} + 2\Delta G_{IU}^{H_2O} \quad (8)$$

The parameter A data are described as the following equation:

$$y = f_N(y_N + m_N[\text{GdnHCl}]) + f_I y_I + f_U(y_U + m_U[\text{GdnHCl}]) \quad (9)$$

where y is the global parameter A data; y_N and y_U are the intercept of the initial, intermediate, and final baselines, respectively. m_N and m_U are the slopes of the initial, intermediate, and final transitions, respectively. y_I represents the fraction of the intermediate calculated by the data, which is assumed not to vary within the transition zone to minimize the number of parameters in the fit. The folding profiles were fitted to eq 9 with the regression wizard of SigmaPlot, followed by the nonlinear least-squares algorithm. The initial parameters were provided, and the regression was run until a minimum R^2 was reached. A fit was judged to be satisfactory by passing of both the normality and constant variance tests.

RESULTS

Multistate Equilibrium Unfolding of βA3-, βB1-, and βA3/βB1-Crystallins. β-Crystallin samples with increasing concentration of GdnHCl were incubated at 4 °C overnight to reach the equilibrium. CD, Trp fluorescence, and ANS were used to monitor the secondary and tertiary structural change during unfolding of βA3-, βB1-, and βA3/βB1-crystallins. The folding of the three proteins was independent of protein concentration, as indicated by the almost indistinguishable transition curves from samples with a protein concentration of 0.2 and 1 mg/mL (data not shown). As shown in Figure 1A, the absolute value of the CD signals increased slightly for all three proteins when the GdnHCl concentration rose from 0 to 1.6 M, which implied that low concentration of GdnHCl could rearrange the structure and induce non-native regular secondary structures. Similar observations have also been reported for the unfolding of the other proteins.[40,43,44] Gradual loss of the regular secondary structures began from 1.6 M GdnHCl and reached the fully denatured state at around 5 M. The transition curve of βA3/βB1-crystallin was very similar to that of βA3-crystallin, except for a faster decrease of the ellipticity at high concentration of GdnHCl.

Each monomer of βA3- and βB1-crystallin contains 10 and 8 Trp residues, respectively, rendering the change of intrinsic Trp fluorescence a sensitive probe of the tertiary structural changes of β-crystallin.[45−47] The maximum emission wavelengths of the Trp

dx.doi.org/10.1021/bi201375p | Biochemistry 2011, 50, 10451−10461

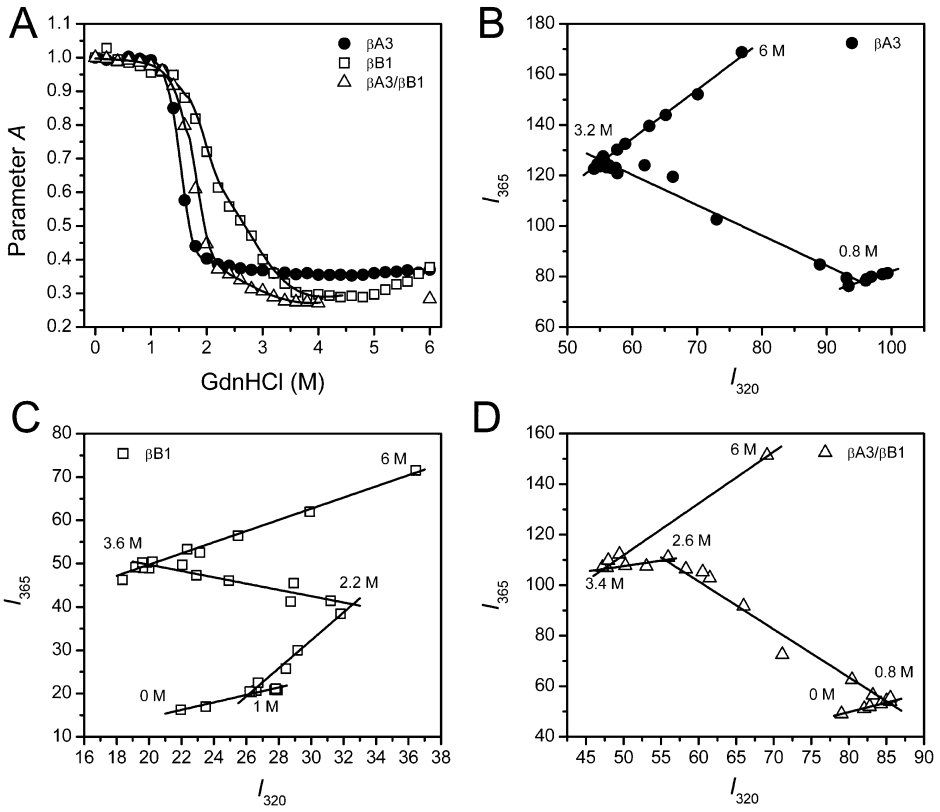

Figure 2. Parameter *A* (A) and phase diagram (B, C, D) analysis of the intrinsic fluorescence spectra of *β*A3- (cycle), *β*B1- (square), and *β*A3/*β*B1-crystallins (triangle) during unfolding. The parameter *A* was obtained by dividing the fluorescence intensity at 320 nm (I_{320}) by that at 365 nm (I_{365}). The phase diagram was constructed by monitoring the changes of I_{365} as a function of I_{320}.

fluorescence (E_{max}) of the native *β*B1- and *β*A3-crystallins were located at 334.5 and 336 nm, while the formation of the heteromer slightly blue-shifted the E_{max} value to about 333 nm. This observation is quite consistent with those in previous publications,[22,31] which suggested that some of the exposed Trp fluorophores became buried in the heteromer. The dependence of the E_{max} on the concentration of GdnHCl clearly revealed the relative stability of the three proteins: *β*B1-crystallin > *β*A3/*β*B1-crystallins > *β*A3-crystallin (Figure 1B). Although the heteromer had a similar behavior to *β*B1-crystallin at low denaturant concentrations, it experienced a much more abrupt transition when GdnHCl concentration rose above 3 M. On the other hand, the heteromer also shows a completely different pattern in the change of emission intensity upon unfolding. The emission intensities of the intrinsic fluorescence of *β*A3- and *β*B1-crystallins slightly decreased and reached a minimum at 1.2 M GdnHCl, while that of *β*A3/*β*B1-crystallin increases by 10% at low GdnHCl concentrations (Figure 1C). The main transition occurred at similar GdnHCl concentrations when monitored by intrinsic fluorescence position or intensity. Interestingly, an additional transition with a significant increase of the Trp fluorescence was observed for all three proteins at high GdnHCl concentrations above 5 M. This phenomenon is seldom observed in previous folding studies. The unfolding states exhibited the maximum emission intrinsic fluorescence intensity, indicating that a significant quenching of the intrinsic fluorescence in the native states of *β*-crystallins. These observations implied that several distinct intermediates might be populated during the unfolding of the three proteins and the unfolding behavior of the heterodimer *β*A3/*β*B1-crystallin could not be simply explained by the sum of its two component monomers.

ANS is a widely used fluorescence probe to monitor the hydrophobic exposure of the proteins.[48] As presented in Figure 1D, the ANS intensity of *β*A3-crystallin reached its maximum at 1.6 M GdnHCl, indicating the existence of an intermediate state with a significant increase in hydrophobic exposure. Notably, the CD signals had only minor changes at 1.6 M GdnHCl, implying the molten globular (MG)-like property of this intermediate state. In contrast, the ANS intensities of *β*B1- and *β*A3/*β*B1-crystallins (especially *β*A3/*β*B1-crystallin) increased to a much smaller extent than that of *β*A3-crystallin. Moreover, the ANS intensity peaks of *β*B1- and *β*A3/*β*B1-crystallins do not agree with a simple transition containing only one intermediate. In fact, more than one intermediate with dissimilar hydrophobic exposure properties might be accumulated at around 1−2 M GdnHCl. Parameter *A* is a precise method to analyze the change in the position and shape of the intrinsic Trp fluorescence spectra.[34] As shown in Figure 2A, the transition curve from parameter *A* of *β*A3-crystallin indicated that the change of the intrinsic fluorescence was a two-stage process involving one intermediate, while *β*B1- and *β*A3/*β*B1-crystallins showed a much more complex pattern. The phase diagram analysis of Trp fluorescence, a sensitive tool to characterize the folding intermediate(s),[35−37,49] was also used to determine the position where the intermediate state(s) appeared. The joint position of lines in the phase diagram indicates the appearance of an intermediate at the corresponding condition. As shown in Figure 2B−D, all of the three proteins showed nonlinear diagrams. Consistent with the above analysis, the folding pathway of the heteromer was similar to that of *β*B1-crystallin but was quite different from that of *β*A3-crystallin. All three proteins had two common intermediates appeared at around 1.0 and 3.4 M GdnHCl, respectively. The major difference was that *β*A3-crystallin

lacked the accumulation of the intermediate between 0.8 and 3.2 M GdnHCl. The absence of this intermediate in the phase diagram of βA3-crystallin might be caused the failure of this method in analyzing irreversible transitions, as suggested by previous researches.[35] Actually, an intermediate of βA3-crystallin appeared at around 1.6 M with the highest ANS fluorescence intensity, the lowest Trp fluorescence intensity, the nearly fully solvent-exposed Trp fluorophores, and the largest CD signal (Figure 1).

To determine the quaternary structural change and the association forms of the intermediates during GdnHCl-induced unfolding, SEC analysis was performed for samples denatured under different concentrations of GdnHCl. The native βA3- and βA3/βB1-crystallin were dominated by the dimeric state in dilute solutions according to the elution volumes, while βB1-crystallin existed in a dimer−monomer equilibrium (Figure 3).

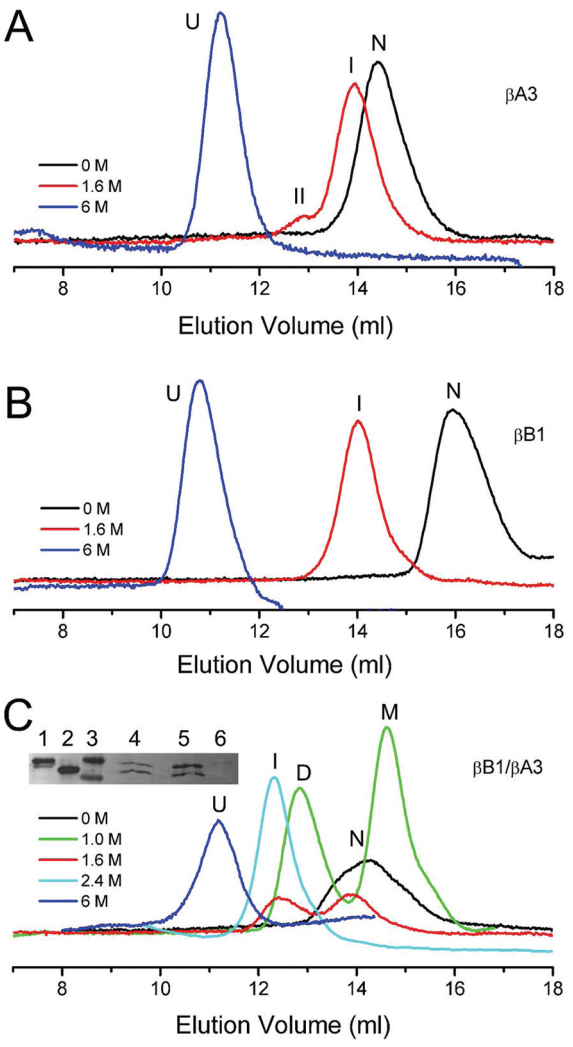

Figure 3. The βA3-, βB1-, and βA3/βB1-crystallins unfolding characterized by SEC and SDS-PAGE analysis. (A) The elution profiles of βA3-crystallin denatured in 0.0, 1.6, and 6.0 M GdnHCl. (B) The elution profiles of βB1-crystallin denatured in 0.0, 1.6, and 6.0 M GdnHCl. (C) The elution profiles of βA3/βB1-crystallin denatured in 0.0, 1.0, 1.6, 2.4, and 6.0 M GdnHCl, respectively. Peaks D, M, and I correspond to the peaks appeared at 1.0 and 2.4 M GdnHCl. The inset shows the identification of eluted samples that collected from the main peaks D, M, and I by SDS-PAGE and silver staining. Bands 1−6 represent βB1-crystallin, βA3-crystallin, marker, D, I, and M, respectively. The void volume of Superdex 200 HR 10/30 column is 8 mL.

This is in good agreement with the previous observations. The SEC analysis was performed under the same conditions for the three proteins to facilitate the identifying of the dissociation of the heteromer. As shown in Figure 3C, both of the 1.0 and 1.6 M profiles of βA3/βB1-crystallin contained two peaks. . As the concentration of GdnHCl rose to 2.4 M, only one elution peak could be observed for βA3/βB1-crystallin. The target peaks were collected and analyzed by SDS-PAGE and silver staining[41] to verify the constitutions of the peaks (inset of Figure 3C). Although the band for peak M was too weak to be detected due to the very low protein concentration, both of the peaks D and M in the 1.0 M profile contained βB1- and βA3-crystallins. Since the elution volume of the native βA3/βB1-crystallin heterodimer was between that of D and M, these two peaks could be assigned as heterodimer and a mixture of βA3- and βB1-crystallin monomer, respectively. As for the 1.6 M profile, the peak eluted at 14 mL occupied at the same position as those of βB1- and βA3-crystallins, indicating that this peak originated from the dissociated βB1- and βA3-crystallin monomers. The single peak in the 2.4 M GdnHCl profile was a mixture of βB1- and βA3-crystallin monomers, suggesting a complete dissociation at this concentration of GdnHCl for all of the three proteins. Similar to previous results,[26,40] herein we also found the gradual decreases of elution volume during unfolding of β-crystallins. This might be caused by the competing effects between dissociation and unfolding, of which one decreased and the other increased the apparent molecular size of the proteins. Nonetheless, βB1- and βA3-crystallins clearly dissociated into monomers at GdnHCl concentrations above 1.6 M, while βA3/βB1-crystallin fully dissociated in 2.4 M GdnHCl.

Partial-Reversible Refolding of βA3-, βB1-, and βA3/βB1-Crystallins. No aggregation was observed during the unfolding of the three proteins. Then the reversibility of GdnHCl-induced unfolding was first monitored by turbidity experiment for the equilibrium refolding protein samples diluted from 6 M to various concentrations of GdnHCl (Figure 4A). Denatured βA3-crystallin formed large amounts of aggregates when diluted to less than 1.4 M GdnHCl, while βB1- and βA3/βB1-crystallins showed little change in the turbidity as the concentration of GdnHCl decreased, especially for βA3/βB1-crystallin. This result suggested that the GdnHCl-induced unfolding of βA3-crystallin was irreversible below 1.4 M GdnHCl, although both βB1 and βA3/βB1-crystallin exhibited a much higher reversible folding process under low GdnHCl concentration conditions. The time-course aggregation kinetics of βA3-crystallin was further examined by diluting the 6 M GdnHCl-denatured samples by different folds. As shown in Figure 4B, no obvious aggregation occurred at GdnHCl concentration higher than 3 M. However, βA3-crystallin showed a slow increase of turbidity when refolded at 2 M GdnHCl, suggesting that the formation of a less stable and aggregation-prone state upon dilution-initiated refolding. Furthermore, aggregation appeared immediately after the manual dilution to GdnHCl concentration less than 2 M, which coincides with the observations in equilibrium refolding experiments.

To further determine the reversibility of β-crystallin folding, the changes of CD, Trp, and ANS fluorescence was monitored during the equilibrium refolding of the fully denatured proteins. As shown in Figure 5, the curves of E_{max} for the unfolding and refolding processes of all three proteins almost overlapped each other when GdnHCl was above 1.5 M. However, they show

dx.doi.org/10.1021/bi201375p | Biochemistry 2011, 50, 10451−10461

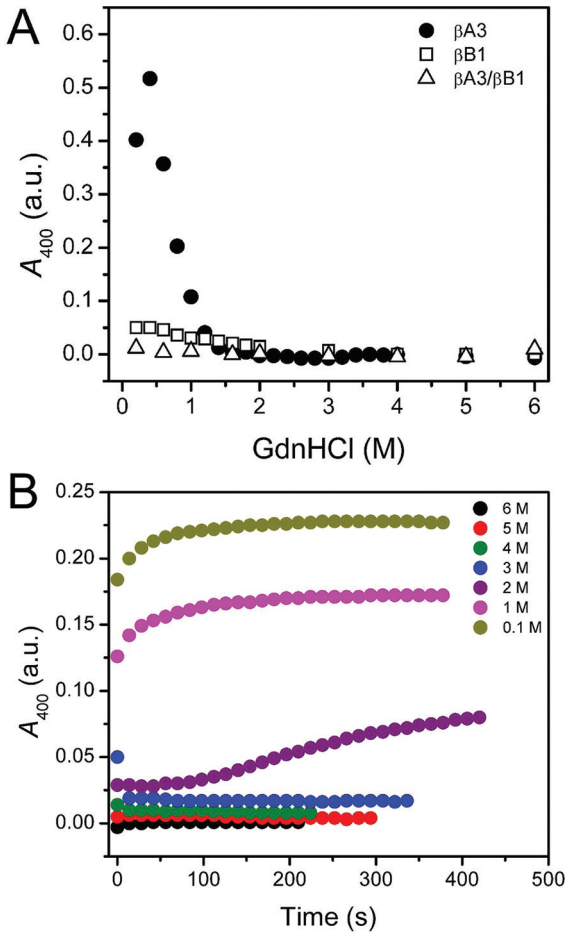

Figure 4. Aggregation of *β*A3-, *β*B1-, and *β*A3/*β*B1-crystallins during refolding monitored by the change of turbidity at 400 nm. (A) Aggregation during equilibrium refolding. The fully denatured protein samples were diluted in buffer A containing various concentrations of GdnHCl and refolded for 20 h at 4 °C. (B) Aggregation during the kinetic refolding of denatured *β*A3-crystallin diluted to various final concentrations (6, 5, 4, 3, 2, 1, and 0.1 M) of GdnHCl.

obvious discrepancies when GdnHCl is below 1.5 M, suggesting that the folding of none of *β*-crystallins was fully reversible. The refolded forms of the three proteins had E_{max} values of 339, 336.5, and 339 nm for *β*A3-, *β*B1-, and *β*A3/*β*B1-crystallins, respectively, about 3 nm red-shifted from the native states. The phase diagrams of the refolding of *β*B1- and *β*A3/*β*B1-crystallins contained the same intermediates as those characterized during unfolding, while that of *β*A3-crystallin had one more intermediate state at 1.4 M GdnHCl (data not shown) than the other two (at 0.8 and 3.2 M GdnHCl) as shown in the unfolding diagram. Notably, this intermediate had been characterized by the ANS fluorescence during the unfolding pathway. Since aggregation greatly affected the fluorescence intensity and CD signal, only the refolding of *β*B1- and *β*A3/*β*B1-crystallins were further analyzed by parameter *A* and CD. The largest discrepancy of the parameter *A* profiles occurred at round 1 M GdnHCl as characterized by the sharp peak (Figure 6A,B), suggesting that this refolding intermediate might be prone to form non-native oligomers. Meanwhile, the ANS fluorescence indicated that the refolded samples contained large hydrophobic exposure (Figure 6C,D).

The above observations suggested that all three proteins refolded partially reversibly although to different extents. Both *β*B1 and *β*A3/*β*B1 could roughly refold into their native conformations after 24 h without any observation of aggregation. A longer refolding time might be able to help these two proteins to achieve the native states more completely. In contrast, the productive refolding of *β*A3-crystallin was significantly competed by the off-pathway aggregation at GdnHCl concentrations below 2 M, indicating that the folding of *β*A3-crystallin was dominated by an irreversible process. Effective chaperones or cofactors are required to facilitate *β*A3-crystallin folding in the physiological conditions.

Prevention of *β*A3-Crystallin against Aggregation during Refolding by *β*B1-Crystallin. The above results indicated that the heteromer did not behave like the mean of the two homomers and revealed that the existence of *β*B1-crystallin could successfully protect *β*A3-crystallin against aggregation during refolding. To verify this proposal, the behavior of *β*A3-crystallin aggregation was studied in the presence of *β*B1-crystallin. As shown in Figure 7, serious aggregation was observed during the refolding of *β*A3-crystallin even at a final protein concentration of 0.1 mg/mL, and no obvious aggregation was found during the kinetic refolding of *β*B1-crystallin. Interestingly, the aggregation of *β*A3-crystallin during kinetic refolding was greatly inhibited by the presence of *β*B1-crystallin in a concentration-dependent manner. It is worth noting that the aggregation-prone intermediate of *β*A3-crystallin appeared at GdnHCl concentrations below 2 M and the refolding of *β*-crystallins was only partially reversible. The results in Figure 7 suggested that the recognition between *β*B1 and *β*A3 was a very fast process that could occur when *β*B1- and/or *β*A3-crystallins were still at the intermediate state. Meanwhile, the addition of the native *β*B1-crystallin had no effect on the aggregation during *β*A3-crystallin refolding (Figure 7). Thus, all our results herein, both the equilibrium

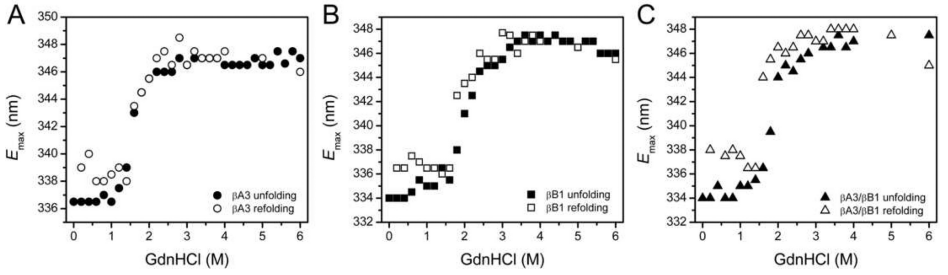

Figure 5. A comparison of the emission maximum wavelength change of the intrinsic fluorescence during unfolding (filled symbols) and refolding (open symbols) of *β*A3- (A), *β*B1- (B), and *β*A3/*β*B1-crystallins (C). For the refolding experiments, the protein was fully denatured in 6 M GdnHCl for 12 h at 4 °C, and then the equilibrium refolding was achieved by dilution of the fully denatured protein into buffer A containing 0.4−5.8 M GdnHCl for 20 h at 4 °C. The final protein concentration was 0.2 mg/mL. All spectroscopic experiments were carried out at 25 °C.

dx.doi.org/10.1021/bi201375p | *Biochemistry* 2011, 50, 10451−10461

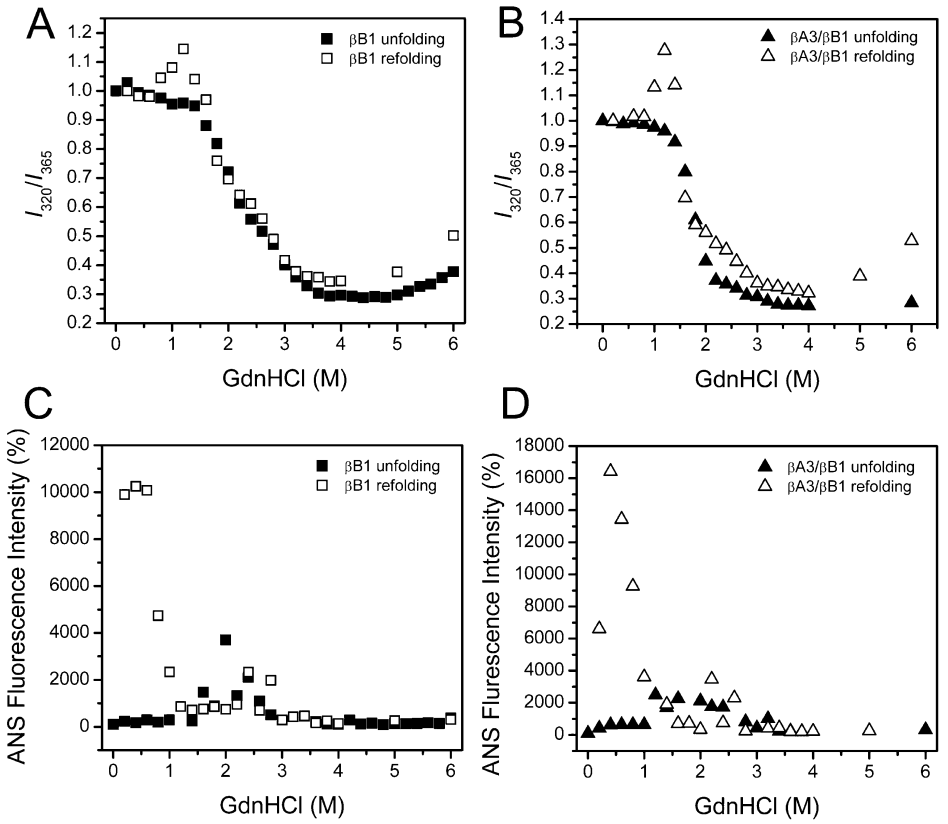

Figure 6. A comparison of the parameter *A* (A, B), ANS fluorescence intensity (C, D), and ellipticity at 222 nm (E, F) changes during the equilibrium refolding of *β*B1- (A, C, E) and *β*A3/*β*B1-crystallins (B, D, F).

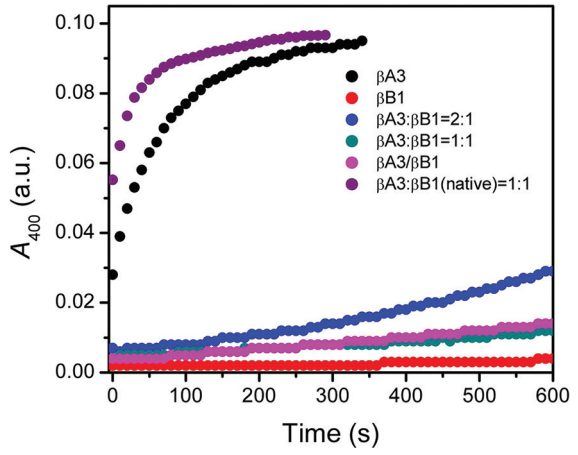

Figure 7. Aggregation during the kinetic refolding of *β*A3-crystallin, *β*B1-crystallin, and the co-refolding of *β*A3- and *β*B1-crystallins with different molar ratios. The protein samples were prepared by diluted the fully denatured proteins in buffer A with a final GdnHCl concentration of 0.2 M and a final protein concentration of 0.1 mg/mL.

and the kinetic refolding, suggested the essential role of *β*B1-crystallin in efficient refolding of *β*A3-crystallin and the ratio dependence of this co-refolding.

DISCUSSION

Multistate Folding of *β*-Crystallins. The *β*- and *γ*-crystallins have highly conserved tertiary structures, containing four Greek-key motifs divided into two domains. The folding of multidomain proteins usually involves the folding of the individual domains and the packing of the domains. The folding of the monomeric two-domain protein *γ*D-crystallin involves an intermediate with an almost intact C-terminal domain and an unfolded N-terminal domain.[27] It is expected that the multimeric two-domain *β*-crystallin might fold via an even more complex pathway. Actually, the folding of the larger oligomer *α*-crystallin has been suggested to undergo a complex pathway involving several intermediates.[16,50−52] Previous studies have proposed that the urea- or GdnHCl-induced unfolding of *β*-crystallins follow either a two-state or a three-state model.[26,29] The folding process of *β*B1-crystallin has been reported to contain more than one intermediate using spin and fluorescence labeling as probes, respectively. However, the probes would also affect the observed folding pathway of proteins.[28] In this research, we used comprehensive spectroscopic analysis and found that both of the *β*-crystallin homomers and heteromer fold via a complex pathway involving several intermediates with distinct structural features.

The possible models of *β*A3-, *β*B1-, and *β*A3/*β*B1-crystallins unfolding/refolding pathway are presented in Scheme 1. All three proteins undergo a multistate folding pathway involving at least three intermediates including one dimeric one (D) and two monomeric ones (I_1 and I_2). It is worth noting that the existence of these intermediates could not be visualized by any single detecting method because every method has its limitations in discovering all folding intermediates. Among the three intermediates, I_2 has been well-characterized to be a common monomeric intermediate for *β*- and *γ*-crystallins. Particularly, folding studies of *β*B2-[26,29] and *γ*D-crystallins[27] revealed that this intermediate contain a less structured N-terminal domain and a well-structured C-terminal domain. Although the present study could not rule out the foldness of

dx.doi.org/10.1021/bi201375p | *Biochemistry* 2011, 50, 10451−10461

Scheme 1. Proposed Folding Mechanisms of *β*A3-, *β*B1-, and *β*A3/*β*B1-Crystallins

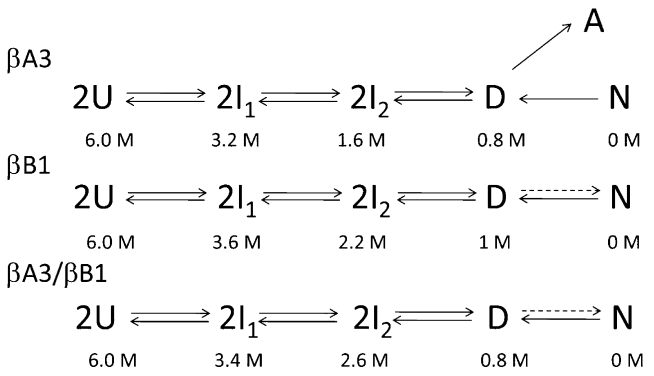

the two domains in I_2 for the three proteins, the structural features suggested that I_2 of *β*B1-crystallin might have similar properties to the intermediate previously characterized in *β*B2- and *γ*D-crystallins, as revealed by about half loss of the native CD signals and partially exposed Trp fluorophores (Figure 8). I_2 of *β*A3-crystallin seemingly possesses dissimilar properties, as characterized by the increased CD signals, partially solvent-exposed Trp residues and large hydrophobic exposure when compared to the native state. At least in some cases, the ANS molecule was characterized to have a high binding affinity to the off-pathway oligomers rather than the surface of the MG state.[53] Although no aggregates was observed during *β*A3-crystallin equilibrium unfolding and refolding at 1.6 M GdnHCl, kinetic studies indicated that this intermediate might form off-pathway oligomers (Figure 4B). Therefore, the unusual behavior of *β*A3-crystallin is possibly caused by the off-pathway oligomers which are undetected in turbidity experiments or quickly exchange with the monomeric intermediate.

The dimeric intermediate D has been characterized in *β*B1-crystallin folding by fluorescence and spin-labeling studies previously.[28] Although protein concentration dependence is characterized in neither our conditions nor those in the previous paper for the unlabeled *β*B1-crystallin, it is significant for the spin-labeled proteins[28] because the narrow protein concentration range appropriate for spectroscopic study is far below that in the lens cell. The structural features of D are close to the native state N (Figure 8), except for a slight rise of the CD signals and reduction of elution volume in the SEC profile (Figure 3). The major difference between D and N is supposed to lie in the molecular shape, which could be affected by the disturbance of dimer cohesion interface and intrasubunit domain interactions as proposed previously in *β*B1-crystallin.[28] The dimeric intermediate is the most aggregation-prone among the three intermediates, as evidenced by the discrepancy between the equilibrium unfolding and refolding curves for all three proteins (Figures 5 and 6). Particularly, the aggregation of *β*A3-crystallin during kinetic refolding is pronounced when the final GdnHCl concentration is below 1 M. Previous study has shown that human *γ*D-crystallin refolds reversibly above 1 M GdnHCl, but aggregates competes with refolding at low concentration of GdnHCl.[28] The final assembly of the domain interactions seems to be critical to both *β*- and *γ*-crystallins. The failure of correctly positioning of the domains will lead to the accumulation of aggregation-prone intermediate and finally to serious aggregation, as has been proved by site-directed mutations in the domain interface of *γ*D-crystallin.[54−56] Thus, the intermediate appearing at low concentrations of denaturants might be crucial to the onset of cataract.

The second monomeric intermediate I_1 has not been characterized for either *β*- or *γ*-crystallins in the literature. I_1 appears at high concentrations of GdnHCl, 3.2, 3.6, and 3.4 M for *β*A3-, *β*B1-, and *β*A3/*β*B1-crystallin, respectively. The E_{max} and ANS binding affinity of I_1 are similar to those of fully unfolded state U at 6 M, suggesting that the Trp fluorophores in I_1 are fully exposed to solvent. The most pronounced difference between I_1 and U lies in the fluorescence intensity, where U has the highest fluorescence intensity among the various states. This suggests that the fluorescence intensity is quenched in N and partially quenched in I_1 and I_2. This phenomenon is also observed in *γ*-crystallins and has been proposed to be a protective mechanism for *γ*-crystallins to escape from UV damage.[57,58] Our findings further suggest that *β*-crystallins might adopt a similar protective mechanism since *β*- and *γ*-crystallins have the same fold in structure. This deduction is also supported by the fact that most residues involved in the fluorescence quenching in *γ*-crystallin are also conserved in *β*-crystallin.

Thermodynamic Parameters of the Three *β*-Crystallins. The equilibrium unfolding curves for E_{max} are best fitted to a two-state model (Figure 1A), possibly because of the inaccuracy of the method to probe the structural changes. Thus, parameter *A* (I_{320}/I_{365}) was chosen to obtain the thermodynamic parameters of the three proteins. For the transition curves from parameter *A*, *β*A3-crystallin is best fitted to two-state models, while those of *β*B1- and *β*A3/*β*B1-crystallins are best fitted to a three-state model (Figure 2A) at GdnHCl concentrations below 4 M. The intermediates I_1 and D were not included in the fitting since the parameter *A* value does not reach its equilibrium at 6 M GdnHCl and therefore cannot identify D. The calculated thermodynamic parameters are presented in Table 1. The total Gibbs free energies of *β*A3-, *β*B1-, and *β*A3/*β*B1-crystallins are similar to that of *β*B2-crystallin.[26] The total Gibbs free energy $\Delta G_{NU}^{H_2O}$ of *β*A3-crystallin

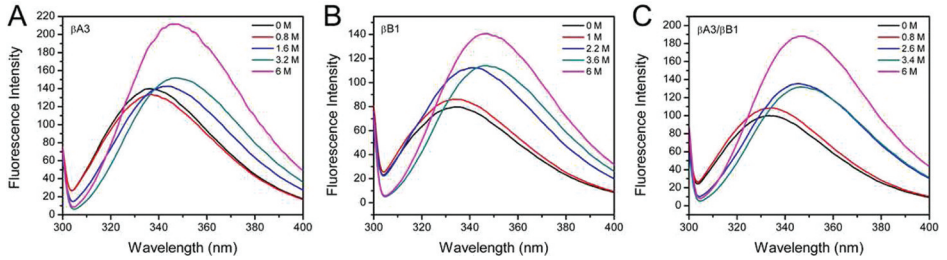

Figure 8. Intrinsic Trp fluorescence spectra of the five states (N, D, I_1, I_2, U) of the three proteins. The protein was incubated in buffer A in the presence of various concentrations of GdnHCl for 12 h at 4 °C. The final protein concentration was 0.2 mg/mL.

Table 1. Thermodynamic Parameters of the Two-State or Three-State Unfolding of β-Crystallins

protein	$\Delta G_{NI}^{H_2O}$ (kJ/mol)	m_{NI} (kJ/(mol M))	$\Delta G_{IU}^{H_2O}$ (kJ/mol)	m_{IU} (kJ/(mol M))	$\Delta G_{NU}^{H_2O}$ (kJ/mol)	m_{NU} (kJ/(mol M))
βA3	61[a]		8[a]		77.0 ± 0.3	14.9 ± 0.1
βB1	74.1 ± 0.7	22.4 ± 0.5	16.2 ± 0.6	5.7 ± 0.1	107 ± 2	
βA3/βB1	74 ± 3	24 ± 2	12 ± 1	4 ± 1	97 ± 5	

[a]Calculated from the values of βB1 and βA3/βB1.

is about 20 kJ/mol lower than that of βA3/βB1-crystallin, which implies that the formation of the heteromer significantly improves the stability of βA3-crystallin. The $\Delta G_{NU}^{H_2O}$ value of βA3/βB1-crystallin is about 10 kJ/mol lower than that of the βB1 homomers (~74.1 kJ/mol). A close inspection of the data listed in Table 1 indicates that the $\Delta G_{NI}^{H_2O}$ value of βA3/βB1-crystallin is almost the same as that of βB1-crystallin, but its $\Delta G_{IU}^{H_2O}$ value was smaller. These results suggest that the subunit interactions of the heterodimer are as strong as that of βB1-crystallin, but the intrasubunit domain interactions are weakened in the heterodimer as reflected by its smaller $\Delta G_{IU}^{H_2O}$. This might be caused by the different packing patterns between the N- and C-terminal domains. The $\Delta G_{IU}^{H_2O}$ value of the heteromer can be estimated by the sum of the stabilities of the two dissociated subunits. If so, the $\Delta G_{NI}^{H_2O}$ and the $\Delta G_{IU}^{H_2O}$ values of βA3-crystallin could be calculated to be ~61 and ~8 kJ/mol, respectively, much smaller than those of βB1- and βA3/βB1-crystallins. Our results are consistent with urea-induced denaturation experiment, which shows that the unfolding curve of βA1/βB1-crystallin shifts to a higher concentration of urea when compared to that of βA1-crystallin, a truncated form of βA3-crystallin.[22]

Folding of βA3-Crystallin Needs the Help of Other Proteins in Lens Cells. The βA3- and βB1-crystallins are both important structural proteins in lens cells. Their packing and association are important in maintaining the transparency and refractive index of the eye lens. Among the β-crystallins, βA3-crystallin has been shown to have a relative lower thermodynamic stability and a higher tendency to aggregate against urea-[22] or heat-induced denaturation.[20] βA3-Crystallin can be successfully protected by βB1-crystallin in the heteromer.[20,22] The modified subunit interactions by point mutations may eliminate this protective effect and contribute to the onset of congenital cataract.[31] Considering that βB1-crystallin gene is expressed early during lens development[12] and βB1-crystallin is the major component in the high-order β-crystallin oligomers in lens,[19] an unresolved problem is whether βB1-crystallin favors the folding of βA3-crystallin. The co-refolding results shown in Figure 7 clearly showed that βB1-crystallin could successfully protect βA3-crystallin against aggregation during co-refolding and thus facilitates the conversion of βA3-crystallin into the native soluble form instead of the aggregation off-pathway product in competition. However, the pre-existed well-folded βB1-crystallin in the refolding buffer could not prevent βA3-crystallin aggregation during the kinetic refolding. The dissimilar effects of the co-refolded and pre-existed βB1-crystallin indicate that the recognition of the subunit interface in heteromer occur either when both proteins are in the folding process or when both are well-folded. The binding sites may be different between the heteromer and homomer, and the exchange rate of the subunit is slow for both β-crystallin heteromer and homomer.[59] Thus, the formation of the heteromer could not be finished during the fast dilution-initiated kinetic refolding. However, this could happen when both proteins are partially folded. The ratio-dependent protection of βA3-crystallin by βB1-crystallin also suggests that the formation of the heteromer is a prior selection during co-refolding.

In mammals, the expression of β-crystallins is under developmental control. Previous studies have shown that βB1-crystallin is prone to form large assemblies while the other β-crystallins are more likely to be dimers, implying the crucial role of βB1-crystallin in the formation and stabilization of the high molecular weight β-crystallin assemblies. Although βB1-crystallin could successfully prevent βA3-crystallin aggregation during co-refolding, the folding of all three proteins is found to be partially reversible. This suggested that the folding to the native state might involve a very slow adjustment process or need the help of the other proteins. Previous studies have shown that α-crystallin, which serves as the main molecular chaperone in the lens,[13] could prevent the unproductive off-pathway aggregation of β-crystallin.[60,61] However, the addition of α-crystallin in the refolding buffer is unable to inhibit βA3-crystallin aggregation during the kinetic refolding [Wang, S., and Yan, Y. B., unpublished data], suggesting that other factors might be responsible for the correct folding of β-crystallins in the newly differentiated lens fiber cells. Nonetheless, it is clear that βB1-crystallin can successfully protect βA3-crystallin in the heteromer. The stronger interaction in the heteromer over those in the homomers prevents βA3-crystallin from stress-induced precipitation and thus allows the other chaperones or foldases to refold them into the native form.

AUTHOR INFORMATION

Corresponding Author

*Tel: +86-10-6278-3477. Fax: +86-10-6277-1597. E-mail: ybyan@tsinghua.edu.cn.

Funding

Funding was provided by the National Key Basic Research and Development (973) Program of China (2010CB912402) and the National Natural Science Foundation of China (No. 30970559).

ABBREVIATIONS

GdnHCl, guanidinium chloride; SDS-PAGE, sodium dodecyl sulfate polyacrylamide gel electrophoresis; ANS, 1-aniline-8-naphthalenesulfonate; CD, circular dichroism; E_m, emission maximum wavelength of intrinsic fluorescence; SEC, size-exclusion chromatography.

REFERENCES

(1) Graw, J. (2009) Genetics of crystallins: cataract and beyond. *Exp. Eye Res. 88*, 173−189.

(2) Hejtmancik, J. F. (2008) Congenital cataracts and their molecular genetics. *Semin. Cell Dev. Biol. 19*, 134−149.

(3) Sharma, K. K., and Santhoshkumar, P. (2009) Lens aging: effects of crystallins. *Biochim. Biophys. Acta 1790*, 1095−1108.

(4) Benedek, G. B. (1971) Theory of transparency of the eye. *Appl. Opt. 10*, 459−473.

(5) Kuszak, J. R., Bertram, B. A., Macsai, M. S., and Rae, J. L. (1984) Sutures of the crystalline lens: a review. *Scanning Electron Microsc.*, 1369−1378.
(6) Bron, A. J., Vrensen, G. F., Koretz, J., Maraini, G., and Harding, J. J. (2000) The ageing lens. *Ophthalmologica 214*, 86−104.
(7) Ueda, Y., Duncan, M. K., and David, L. L. (2002) Lens proteomics: The accumulation of Crystallin modifications in the mouse lens with age. *Invest. Ophth. Vis. Sci. 43*, 205−215.
(8) Piatigorsky, J. (1989) Lens crystallins and their genes - diversity and tissue-specific expression. *FASEB J. 3*, 1933−1940.
(9) Graw, J. (1997) The crystallins: genes, proteins and diseases. *Biol. Chem. 378*, 1331−1348.
(10) Andley, U. P. (2007) Crystallins in the eye: Function and pathology. *Prog. Retin. Eye Res. 26*, 78−98.
(11) Tholozan, F. M. D., and Quinlan, R. A. (2007) Lens cells: More than meets the eye. *Int. J. Biochem. Cell Biol. 39*, 1754−1759.
(12) Bloemendal, H., de Jong, W., Jaenicke, R., Lubsen, N. H., Slingsby, C., and Tardieu, A. (2004) Ageing and vision: structure, stability and function of lens crystallins. *Prog. Biophys. Mol. Biol. 86*, 407−485.
(13) Horwitz, J. (1992) α-Crystallin can function as a molecular chaperone. *Proc. Natl. Acad. Sci. U. S. A. 89*, 10449−10453.
(14) Horwitz, J. (2003) α-Crystallin. *Exp. Eye Res. 76*, 145−153.
(15) Hejtmancik, J. F., Wingfield, P. T., and Sergeev, Y. V. (2004) β-Crystallin association. *Exp. Eye Res. 79*, 377−383.
(16) Pang, M., Su, J. T., Feng, S., Tang, Z. W., Gu, F., Zhang, M., Ma, X., and Yan, Y. B. (2010) Effects of congenital cataract mutation R116H on alphaA-Crystallin structure, function and stability. *Biochim. Biophys. Acta 1804*, 948−956.
(17) Zhang, W., Cai, H.-C., Li, F.-F., Xi, Y.-B., Ma, X., and Yan, Y.-B. (2011) The congenital cataract-linked G61C mutation destabilizes γD-Crystallin and promotes non-native aggregation. *PLoS One 6*, e20564.
(18) Chan, M. P., Dolinska, M., Sergeev, Y. V., Wingfield, P. T., and Hejtmancik, J. F. (2008) Association properties of βB1- and βA3-crystallins: ability to form heterotetramers. *Biochemistry 47*, 11062−11069.
(19) Bateman, O. A., Lubsen, N. H., and Slingsby, C. (2001) Association behaviour of human βB1-Crystallin and its truncated forms. *Exp. Eye Res. 73*, 321−331.
(20) Srivastava, K., Gupta, R., Chaves, J. M., and Srivastava, O. P. (2009) Truncated human βB1-Crystallin shows altered structural properties and interaction with human βA3-Crystallin. *Biochemistry 48*, 7179−7189.
(21) Zigler, J. S. Jr., Zhang, C., Grebe, R., Sehrawat, G., Hackler, L. Jr., Adhya, S., Hose, S., McLeod, D. S., Bhutto, I., Barbour, W., Parthasarathy, G., Zack, D. J., Sergeev, Y., Lutty, G. A., Handa, J. T., and Sinha, D. (2011) Mutation in the βA3/A1-Crystallin gene impairs phagosome degradation in the retinal pigmented epithelium of the rat. *J. Cell. Sci. 124*, 523−531.
(22) Bateman, O. A., Sarra, R., van Genesen, S. T., Kappe, G., Lubsen, N. H., and Slingsby, C. (2003) The stability of human acidic β-Crystallin oligomers and hetero-oligomers. *Exp. Eye Res. 77*, 409−422.
(23) Bax, B., Lapatto, R., Nalini, V., Driessen, H., Lindley, P. F., Mahadevan, D., Blundell, T. L., and Slingsby, C. (1990) X-ray analysis of βB2-Crystallin and evolution of oligomeric lens proteins. *Nature 347*, 776−780.
(24) Jung, J., Byeon, I. J., Wang, Y., King, J., and Gronenborn, A. M. (2009) The structure of the cataract-causing P23T mutant of human γD-Crystallin exhibits distinctive local conformational and dynamic changes. *Biochemistry 48*, 2597−2609.
(25) Van Montfort, R. L., Bateman, O. A., Lubsen, N. H., and Slingsby, C. (2003) Crystal structure of truncated human βB1-Crystallin. *Protein Sci. 12*, 2606−2612.
(26) Fu, L., and Liang, J. J. (2002) Unfolding of human lens recombinant βB2- and γC-crystallins. *J. Struct. Biol. 139*, 191−198.
(27) Kosinski-Collins, M. S., and King, J. (2003) In vitro unfolding, refolding, and polymerization of human γD Crystallin, a protein involved in cataract formation. *Protein Sci. 12*, 480−490.
(28) Koteiche, H. A., Kumar, M. S., and McHaourab, H. S. (2007) Analysis of βB1-Crystallin unfolding equilibrium by spin and fluorescence labeling: evidence of a dimeric intermediate. *FEBS Lett. 581*, 1933−1938.
(29) Wieligmann, K., Mayr, E. M., and Jaenicke, R. (1999) Folding and self-assembly of the domains of βB2-Crystallin from rat eye lens. *J. Mol. Biol. 286*, 989−994.
(30) Gupta, R., Chen, J., and Srivastava, O. P. (2010) A serine-type protease activity of human lens βA3-Crystallin is responsible for its autodegradation. *Mol. Vis. 16*, 2242−2252.
(31) Wang, K. J., Wang, S., Cao, N. Q., Yan, Y. B., and Zhu, S. Q. (2011) A novel mutation in *CRYBB1* associated with congenital cataract-microcornea syndrome: the p.Ser129Arg mutation destabilizes the βB1/βA3-Crystallin heteromer but not the βB1-Crystallin homomer. *Hum. Mutat. 32*, E2050−E2060.
(32) Bradford, M. M. (1976) A rapid and sensitive method for the quantitation of microgram quantities of protein utilizing the principle of protein-dye binding. *Anal. Biochem. 72*, 248−254.
(33) Turoverov, K. K., Haitlina, S. Y., and Pinaev, G. P. (1976) Ultraviolet fluorescence of actin. Determination of native actin content in actin preparations. *FEBS Lett. 62*, 4−6.
(34) Miller, D. L., and Schildbach, J. F. (2003) Evidence for a Monomeric Intermediate in the Reversible Unfolding of F Factor TraM. *J. Biol. Chem. 278*, 10400−10407.
(35) Bushmarina, N. A., Kuznetsova, I. M., Biktashev, A. G., Turoverov, K. K., and Uversky, V. N. (2001) Partially folded conformations in the folding pathway of bovine carbonic anhydrase II: a fluorescence spectroscopic analysis. *ChemBioChem 2*, 813−821.
(36) He, H.-W., Zhang, J., Zhou, H.-M., and Yan, Y.-B. (2005) Conformational Change in the C-Terminal Domain Is Responsible for the Initiation of Creatine Kinase Thermal Aggregation. *Biophys. J. 89*, 2650−2658.
(37) Su, J.-T., Kim, S.-H., and Yan, Y.-B. (2007) Dissecting the pretransitional conformational changes in aminoacylase I thermal denaturation. *Biophys. J. 92*, 578−587.
(38) Jiang, Y., Yan, Y.-B., and Zhou, H.-M. (2006) Polyvinylpyrrolidone 40 assists the refolding of bovine carbonic anhydrase B by accelerating the refolding of the first molten globule intermediate. *J. Biol. Chem. 281*, 9058−9065.
(39) Kurganov, B. I. (2002) Kinetics of protein aggregation. Quantitative estimation of the chaperone-like activity in test-systems based on suppression of protein aggregation. *Biochemistry (Moscow) 67*, 409−422.
(40) Wang, S., Liu, W. F., He, Y. Z., Zhang, A., Huang, L., Dong, Z. Y., and Yan, Y. B. (2008) Multistate folding of a hyperthermostable Fe-superoxide dismutase (TcSOD) in guanidinium hydrochloride: The importance of the quaternary structure. *Biochim. Biophys. Acta 1784*, 445−454.
(41) Switzer, R. C. III, Merril, C. R., and Shifrin, S. (1979) A highly sensitive silver stain for detecting proteins and peptides in polyacrylamide gels. *Anal. Biochem. 98*, 231−237.
(42) Ke, H., Zhang, S., Li, J., Howlett, G. J., and Wang, C. C. (2006) Folding of Escherichia coli DsbC: characterization of a monomeric folding intermediate. *Biochemistry 45*, 15100−15110.
(43) Hagihara, Y., Aimoto, S., Fink, A. L., and Goto, Y. (1993) Guanidine hydrochloride-induced folding of proteins. *J. Mol. Biol. 231*, 180−184.
(44) He, G.-J., Zhang, A., Liu, W.-F., Cheng, Y., and Yan, Y.-B. (2009) Conformational stability and multistate unfolding of poly(A)-specific ribonuclease. *FEBS J. 276*, 2849−2860.
(45) Burstein, E. A., Abornev, S. M., and Reshetnyak, Y. K. (2001) Decomposition of protein tryptophan fluorescence spectra into log-normal components. I. Decomposition algorithms. *Biophys. J. 81*, 1699−1709.
(46) Reshetnyak, Y. K., and Burstein, E. A. (2001) Decomposition of protein tryptophan fluorescence spectra into log-normal components. II. The statistical proof of discreteness of tryptophan classes in proteins. *Biophys. J. 81*, 1710−1734.

(47) Reshetnyak, Y. K., Koshevnik, Y., and Burstein, E. A. (2001) Decomposition of protein tryptophan fluorescence spectra into log-normal components. III. Correlation between fluorescence and microenvironment parameters of individual tryptophan residues. *Biophys. J. 81*, 1735−1758.
(48) Rosen, C. G., and Weber, G. (1969) Dimer formation from 1-amino-8-naphthalenesulfonate catalyzed by bovine serum albumin. A new fluorescent molecule with exceptional binding properties. *Biochemistry 8*, 3915−3920.
(49) Georlette, D., Blaise, V., Dohmen, C., Bouillenne, F., Damien, B., Depiereux, E., Gerday, C., Uversky, V. N., and Feller, a. G. (2003) Cofactor Binding Modulates the Conformational Stabilities and Unfolding Patterns of NAD-dependent DNA Ligases from *Escherichia coli* and *Thermus scotoductus*. *J. Biol. Chem. 278*, 49945−49953.
(50) Raman, B., Ramakrishna, T., and Rao, C. M. (1995) Rapid refolding studies on the chaperone-like α-Crystallin. Effect of α-Crystallin on refolding of β- and γ-crystallins. *J. Biol. Chem. 270*, 19888−19892.
(51) Doss-Pepe, E. W., Carew, E. L., and Koretz, J. F. (1998) Studies of the denaturation patterns of bovine α-Crystallin using an ionic denaturant, guanidine hydrochloride and a non-ionic denaturant, urea. *Exp. Eye Res. 67*, 657−679.
(52) Sun, T.-X., Akhtar, N. J., and Liang, J. J. N. (1999) Thermodynamic stability of human lens recombinant αA- and αB-crystallins. *J. Biol. Chem. 274*, 34067−34071.
(53) Povarova, O. I., Kuznetsova, I. M., and Turoverov, K. K. (2010) Differences in the pathways of proteins unfolding induced by urea and guanidine hydrochloride: molten globule state and aggregates. *PLoS One 5*, e15035.
(54) Flaugh, S. L., Kosinski-Collins, M. S., and King, J. (2005) Interdomain side-chain interactions in human γD Crystallin influencing folding and stability. *Protein Sci. 14*, 2030−2043.
(55) Flaugh, S. L., Kosinski-Collins, M. S., and King, J. (2005) Contributions of hydrophobic domain interface interactions to the folding and stability of human γD-Crystallin. *Protein Sci. 14*, 569−581.
(56) Das, P., King, J. A., and Zhou, R. (2010) β-strand interactions at the domain interface critical for the stability of human lens γD-Crystallin. *Protein Sci. 19*, 131−140.
(57) Chen, J., Toptygin, D., Brand, L., and King, J. (2008) Mechanism of the efficient tryptophan fluorescence quenching in human γD-Crystallin studied by time-resolved fluorescence. *Biochemistry 47*, 10705−10721.
(58) Chen, J., Callis, P. R., and King, J. (2009) Mechanism of the very efficient quenching of tryptophan fluorescence in human γD- and γS-crystallins: the γ-Crystallin fold may have evolved to protect tryptophan residues from ultraviolet photodamage. *Biochemistry 48*, 3708−3716.
(59) Sergeev, Y. V., Dolinska, M. B., Chan, M. P., Palmer, I., and Wingfield, P. T. (2009) N-Terminal Extension of βB1-Crystallin: Identification of a Critical Region That Modulates Protein Interaction with βA3-Crystallin. *Biochemistry 48*, 9684−9695.
(60) Wang, K. Y., and Spector, A. (1994) The chaperone activity of bovine α-Crystallin - interaction with other lens crystallins in native and denatured states. *J. Biol. Chem. 269*, 13601−13608.
(61) Michiel, M., Duprat, E., Skouri-Panet, F., Lampi, J. A., Tardieu, A., Lampi, K. J., and Finet, S. (2010) Aggregation of deamidated human βB2-Crystallin and incomplete rescue by α-Crystallin chaperone. *Exp. Eye Res. 90*, 688−698.